CIRCULARLY POLARIZED MECHANICAL RESONANCES

Pen-Li Yu and Sunil A. Bhave
OxideMEMS Lab, Purdue University, West Lafayette, Indiana, USA

ABSTRACT

We demonstrate a new type of rotational resonance, circularly-polarized mechanical resonance (CPMR), where a normal mode of a circular membrane revolves around its center. Clockwise or counter-clockwise full-angle rotation of normal mode is observed in circular membranes with a diameter of 710 μm or 960 μm and a thickness of 15 μm. We measure the (1,1) and higher order CPMR resonances with rates up to 5.3 million revolutions/second.

INTRODUCTION

Generating large and stable angular momentum at microscale has applications in spinning-mass MEMS gyroscopes, precision rotation stages, and micro-motors. Ultrasonic motors rely on nonlinear bifurcation of the stator's mode to cause rotation [1], while electrowetting requires complicated assembly [2], and levitation demands large, perfectly symmetric voltages [3,4]. Circular movement of nano-cantilever requires large vibration amplitude beyond "classical" Duffing regime [5,6].

Our discovery of CPMR provides a novel and simple way to generate large angular velocity. The excitation of CPMR only requires an axial piezo actuator and a sinusoidal tone. It is operated in the linear regime with no threshold. A rotation rate of 33.5 million radians per second for a higher order mode is observed. The range of mode frequencies is only limited by the bandwidth of our piezoelectric transducer.

RESONATORS AND EXPERIMENTAL SETUP

Fig. 1 (a) and (b) illustrate the fabrication process of the membranes. We carry out deep reactive ion etch (DRIE) on the backside of 4H SiC wafers [7,8]. By timing the etching, suspended circular membrane resonators are fabricated. The process is like backside release process except there is no stop layer. The membrane has a diameter of 710 μm or 960 μm and thickness of 15 μm. The thickness of the membrane is determined by measuring the depth of the trench [Fig. 1 (c)]. A photograph of the diaphragm chip is shown in Fig. 1 (d).

We employ a scanning Laser Doppler Vibrometer (LDV, Polytec MSA-400) to characterize mechanical motion [9,10]. The apparatus is located on a vibration isolation slab that meets NIST-A1 vibration standards. The membrane is bonded to the edge of an axial piezo actuator [Fig. 2 (a)]. The laser beam of the interferometer is focused through a 5× microscope objective and incident normal to the membrane plane. The laser wavelength is 633 nm, and the laser power is less than 1 mW. We raster scan the laser spot over ~ 1000 points on the membrane and measure frequency and time-domain responses at each point. We drive the piezo actuator with a broadband, pseudo-random excitation and perform Fast-Fourier Transform (FFT) to construct frequency spectrum. Alternatively, we can drive the piezo actuator with a single-tone, sinusoidal excitation, and measure the membrane displacement as a function of time. The velocity resolution is less than 1 um/s which corresponds to a displacement resolution of < 1 pm at 1 MHz.

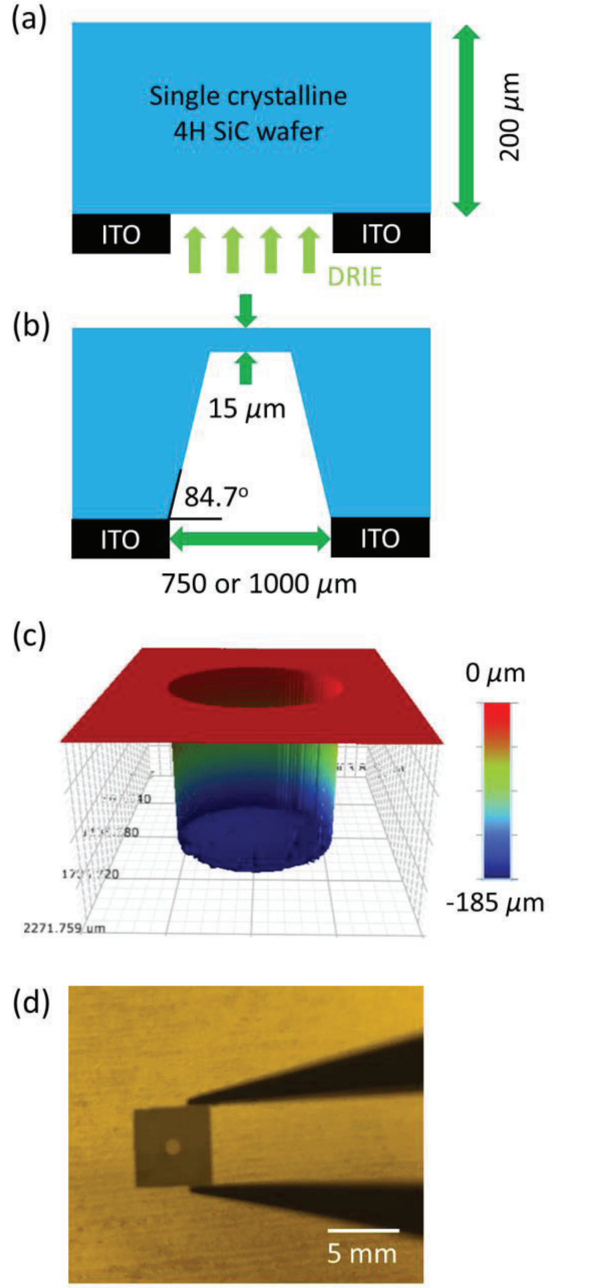

Figure 1: (a)-(b) Timed DRIE of 4H SiC to fabricate suspended membrane resonators [7,8]. Indium Tin Oxide (ITO) is used as a hard mask. 84.7° sidewall is achieved. (c) A DRIE trench profile measured by a 3-dimensional optical profiler (GT-K). The thickness of the membrane is obtained by subtracting the depth of the trench from the chip thickness. (d) Photograph of the diaphragm chip. The 5-mm square chip has a 15 μm thin membrane which looks like a pinhole because it is transparent to visible light. The membrane diameter is 960 μm.

978-1-940470-03-0/HH2018/$25©2018TRF
DOI 10.31438/trf.hh2018.58

RESULTS

Fig. 2 shows the measured displacement spectra of a 960 μm diameter membrane. We first measure the broadband displacement spectrum over 0-5 MHz. Many membrane modes are observed [7]. Their mode shapes and resonant frequencies are consistent with COMSOL simulation to within 4%. Next, we do a fine scan of the displacement spectra near the (1,1) mode. We observe the normal modes and two CPMR (1,1) modes at 746 kHz and 790 kHz with clockwise and counterclockwise revolutions. Table 1 shows the measured timestamps of the CPMRs observed in Fig. 2 (c) and many higher order CPMRs of a 710 μm diameter membrane. The CPMR modes complete one revolution in a period $T = 1/f$, where f is the excitation frequency. In 1 second, the (1,1) CPMR mode completes 746000 revolutions, while the (2,2) CPMR mode of the 710 μm membrane completes 5.3 million revolutions.

We also plot the time-average mode shape in the last column of Table 1. In contrast to the normal modes, the time-average mode shape of CPMRs show circular symmetry, as expected from the revolutions. A distinct feature of CPMR is that the location of maximum displacement travels around the membrane. Each point reaches its maximum displacement at a time corresponding to its angular position on the membrane plane. We perform time-domain measurements at 6 locations equidistant from the center [Fig. 3. (a)]. At 763 kHz, all points reach their maximum and minimum points concurrently, as is expected for a normal mode [Fig. 3 (b)]. Fig. 3 (c) shows the displacements as function of time for the (1,1) clockwise CPMR mode. In contrast to Fig. 3 (b), points at smaller angular position reach maximum displacement later, leading to clockwise rotation.

Up to the resolution of the LDV, we do not observe any "onset" or threshold point for the revolution. We measure a linear relationship between drive amplitude and piezo stimulus up to the maximum voltage allowed by the LDV system [Fig. 4(a)]. The CPMR does not arise from nonlinear model coupling [1,5,6].

Operating at the resonant peak [blue line in Fig. 4(b)] gives us almost perfect traveling wave revolution. However, the amplitudes are not exactly uniform throughout the rotation, as shown by the time-averaged mode shape and Fig.3 (c). By operating at 10 kHz off the resonance [purple line in Fig. 4(b)], we observe a perfectly smooth revolution [see legends of Fig. 4 (b)]. The difference between on and off-peak response indicates that the CPMR is not an eigenmode of the membrane, but a superposition of eigenmodes that is perfectly balanced in amplitude and phase.

DISCUSSION

Here we provide a mathematical framework to describe the CPMR. We model CPMRs as the excitation of two spatially orthogonal normal modes with out-of-phase oscillations (See Fig. 5 for a visual illustration). To be more precise, we start with the general solutions $u_{mn}(r, \theta, t)$ of the vibrating drum head:

$$(A \cos c\lambda_{mn}t + B \sin c\lambda_{mn}t) J_m(\lambda_{mn}r)(C \cos m\theta + D \sin m\theta),$$

where $J_m(\lambda_{mn}r)$ is the Bessel function, $\lambda_{mn} = \alpha_{mn}/a$, α_{mn} is the n-th positive root of J_m, a is the radius of the membrane, *and* c is the wave speed. The Bessel function and index m define the number of nodal circles. The index m defines the number of nodal diameters. Constants C and D define the mode orientation, while constants A and B define the phase relation between the driving voltage and displacement. The two spatially orthogonal normal modes are described by two solutions with same indices m and n, but with $(C, D) = (0,1)$ and $(1,0)$, respectively (See Fig. 5). When these two modes oscillate out of phase, that is, the first mode oscillates as $\cos c\lambda_{mn}t$ $[(A, B) = (1,0)]$ while the second mode oscillates as $\sin c\lambda_{mn}t$ $[(A, B) = (0,1)]$, the superposition of these two modes generates full-angle counterclockwise rotation in one period of oscillation. On the other hand, if the first mode oscillates as $\sin c\lambda_{mn}t$ and the second mode oscillates as $\cos c\lambda_{mn}t$, the superposition of these two modes lead to clockwise rotation. Exact source of out-of-phase signaling is currently under investigation.

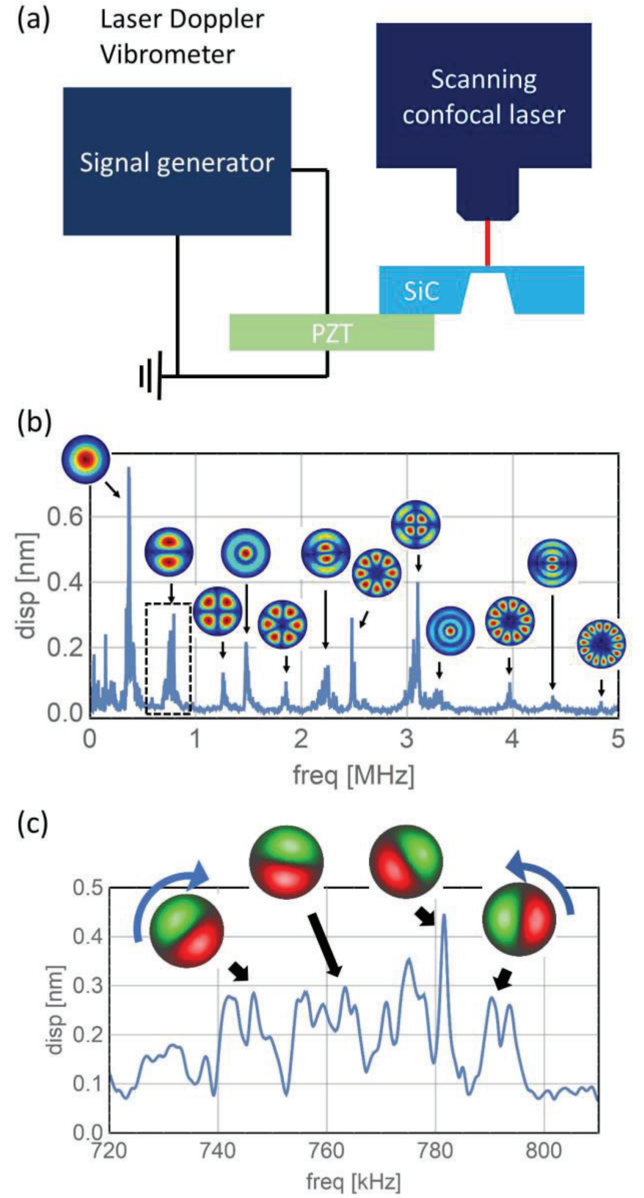

Figure 2: (a) LDV measurement setup with one key caveat — the sample is glued to the PZT at the edge of the actuator. The laser is raster scan over ~1000 points on the membranes. (b) Displacement spectrum of a 960 μm *membrane in 0-5 MHz range measured by the LDV in FFT mode. [Picture and plot are reproduced from [7] to provide context to] (c) Fine scan of the displacement spectrum around the (1,1) normal mode at 780 kHz. The CPMR modes are on either side of the normal modes.*

Table 1: Measured timestamps of the normal (1,1) mode (second row) compared to the (1,1) and higher order CPMR resonances. Two membranes with diameters of 960 µm and 710 µm are measured. *CPMR with rate up to* 5.3 million revolutions/second is observed. The period T is given by $T = 1/f$. *The time-average mode shapes (last column) for the CPMR modes have circular symmetry because of revolution.*

Dia. [mm]	**Mode**	***f* [MHz]**	**Direction**
0.96	(1,1)	0.763	---
0.96	(1,1)	0.746	
0.96	(1,1)	0.789	
0.71	(1,1)	1.397	
0.71	(2,1)	2.263	
0.71	(3,1)	3.260	
0.71	(1,2)	3.875	
0.71	(2,2)	5.326	

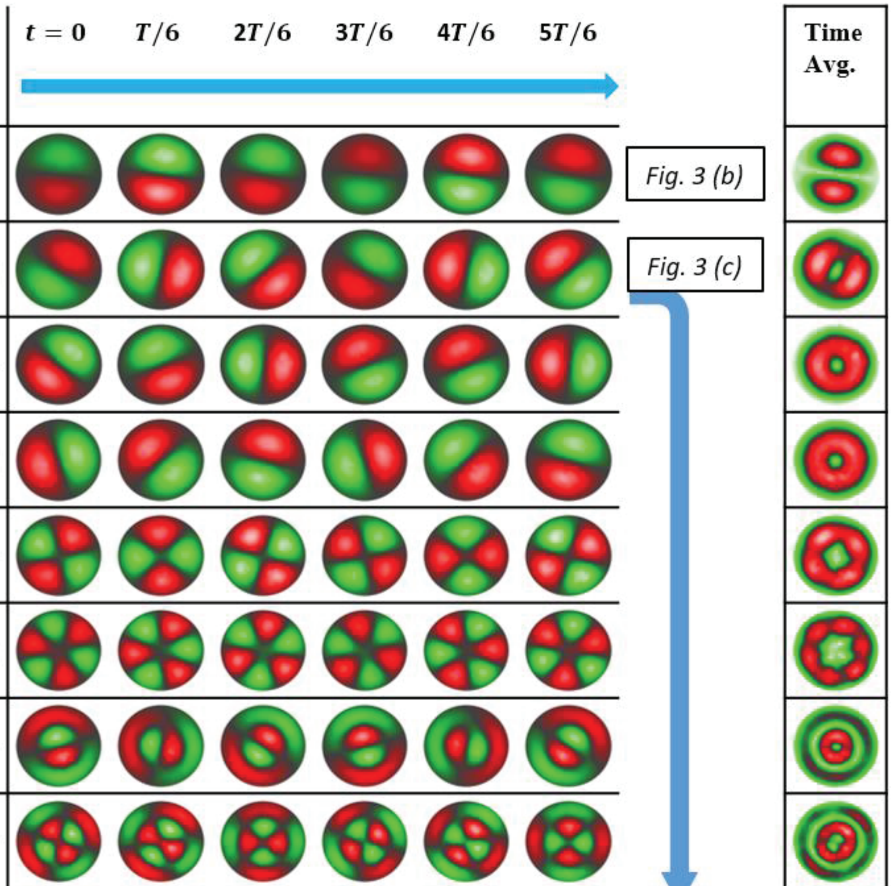

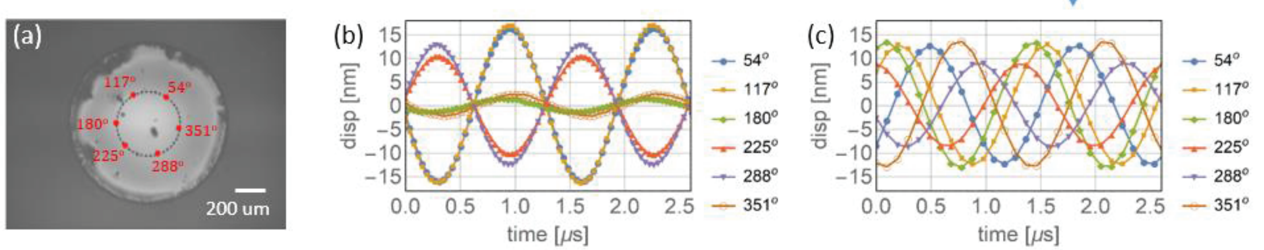

Figure 3: The vibration phase is the most distinctive feature of the CPMR modes. (a) We positioned laser spots on six points to measure their displacement as a function of time with respect to the drive (3 Volt). (b) For the normal mode, all points vibrate coherently. They reach their amplitude maximum and minimum at the same time. (c) For the CPMR mode, consecutive points reach maximum displacement with 60º phase delay. There is no instant in time where all points have zero displacement, as seen in Fig. 3(b) at 0.6 µs.

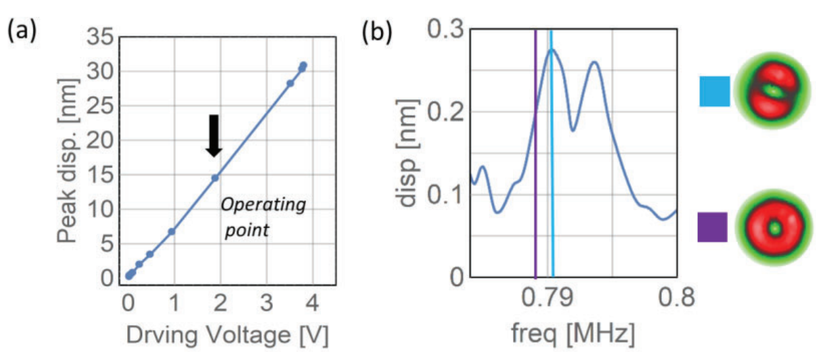

Figure 4: (a) *The membrane vibrates in the linear regime. The peak displacement of the (1,1) CPMR mode at 1.397 MHz as a function of driving voltage. (b) Time-average deflection shapes at the excitation frequencies. A perfectly smooth revolution (with circular symmetry) is achieved by driving 10 kHz off resonance (purple line).*

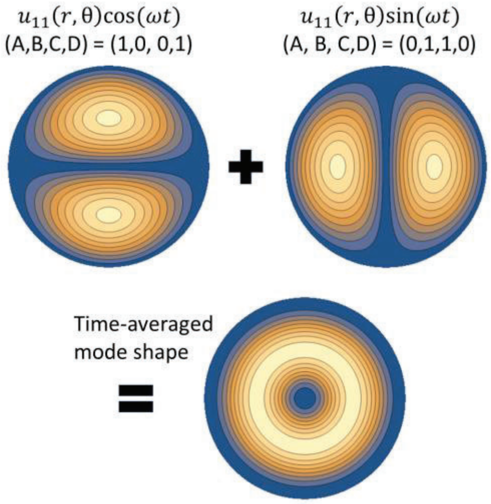

Figure 5: *Illustration of a mathematical model for CPMR. Two spatially-orthogonal normal modes (upper left and upper right) oscillating out of phase leads to CPMR. The rotation direction depends on the A, B, C, D coefficients.*

In conclusion, we present the observation of CPMRs in microfabricated membranes. We measure normal modes revolving under single tone excitation from an axial piezo actuator. CPMRs undergo full-angle, ultra-fast rotation (the mode rotates, not the resonator) and can be selectively biased to revolve clockwise or counter-clockwise rotational direction. We measure the (1,1) and higher order CPMR resonances with rates up to 33.5 million radians per second. The CPMR modes complete one revolution in one period of oscillation. We model the CPMR as a superpositions of two normal modes with out-of-phase vibrations. The direction of vibration is determined by the relative phase of the two modes.

ACKNOWLEDGEMENTS

We thank Devin Kalafut, Conor Pyles, and Sen Dai for technical assistance in LDV setup. This work was supported by AFOSR MURI grant. We thank M. M. Torunbalci, A. Bhat, and Y. He, and T.-H. Chang for discussions.

REFERENCES

[1] S. Tin, M. Pandey, and A. Lal, "Experimental Verification and Characterization of Sub-Harmonic Traveling Wave on an Ultrasonic Micromotor", Ultrasonics Symposium 2010, San Diego, California, USA, October 11-14, 2010, pp. 1841-1844.

[2] G. Sun, T. Liu, P. Sen, W. Shen, C. Gudeman, and C.-J. Kim, "Electrostatic Side-Drive Rotary Stage on Liquid-Ring Bearing", J. MEMS, 23 (2013), pp. 147-156.

[3] S. Nakamura, "MEMS inertial sensor toward higher accuracy & multi-axis sensing", IEEE Sensors 2005, Irvine, CA, USA, Oct. 30-Nov. 3, 2005, pp. 939-942.

[4] B. Damrongsak and M. Kraft, "A micromachined Electrostatically Suspended Gyroscope with Digital Force Feedback", IEEE Sensors 2005, Irvine, CA, USA, Oct. 30-Nov. 3, 2005, pp. 401-404.

[5] S. Perisanu., T. Barois, A. Ayari, P. Poncharal, M. Choueib, S. T. Purcell, and P. Vincent, "Beyond the linear and Duffing regimes in nanomechanics: Circularly polarized mechanical resonances of nanocantilevers", Phy. Rev. B 81, 165440 (2010).

[6] W. G. Conley, A. Raman, C. M. Krousgrill, and S. Mohammadi, "Nonlinear and Nonplanar dynamics of Suspended Nanotube and Nanowire Resonators", Nano Lett., 2008, 8 (6), pp. 1590-1595.

[7] P. -L. Yu, N. Opondo, S. Dai, B. Jiang, D. T. Morisette, and S. A. Bhave, "Single Crystalline 4H SiC Membrane Resonators", IEEE International Frequency Control Symposium 2018, Olympic Valley, CA, USA, May 21-24, 2018.

[8] S. -D. Ko, B. Hamelin, J. Yang, and F. Ayazi, "High-Q Monocrystalline Silicon Carbide Disk Resonators Fabricated Using DRIE of Thick SiC-on-Insulator Substrates", MEMS 2018, Belfast, UK, Jan. 21-25, 2018, pp. 996-999.

[9] J. F. Portoles, P. J. Cumpson, J. Hedley, S. Allen, P. M. Williams, and S. J. B. Tendler, "Accurate velocity measurements of AFM-cantilever vibrations by Doppler interferometry", J. Exp. Nanosci., 2006, 1:1, 51-52.

[10] L. B. Biedermann, R. C. Tung, A. Raman, R. G. Reifenberger, "Flexural vibration spectra of carbon nanotubes measured using laser Doppler vibrometry", Nanotechnology 20 (2009) 035702.

CONTACT

*Pen-Li (Ben) Yu, tel: +1-765-430-6400; yu586@purdue.edu